Proceedings of the IASS Annual Symposium 2016
"Spatial Structures in the 21st Century"
26-30 September, 2016, Tokyo, Japan
K. Kawaguchi, M. Ohsaki, T. Takeuchi (eds.)

Shape optimization of latticed shells consisting of ruled surface

Shinnosuke FUJITA*, Makoto OHSAKI[a], and Kazuya SEKI[b]

*Assistant Professor, UDPRC (Former SERC), Tokyo Institute of Technology, Dr. Eng.
Nagatsuta-chou 4259, Midori-ku, Yokohama 226-8503, Japan
Email : fujita.s.ag@m.titech.ac.jp

[a]Professor, Dept. of Architecture and Architectural Eng., Kyoto University, Dr. Eng.
[b]Azusa Sekkei, Former Graduate Student, Hiroshima University, M. Eng

Abstract

A shape optimization method is presented for latticed shells using ruled surface. Boundary shape is defined using two Bézier curves, and the points with the same parameter value are connected by a line to model a ruled surface. The locations of control points of the Bézier curves are considered as design variables of the optimization problem. This way, the number of variables for optimization can be drastically reduced without sacrificing smoothness and complexity of the surface. The total strain energy is minimized under constraints on material volume. In this optimization problem, not only vertical loads but also horizontal loads are considered. While the optimal shape is expected to have a large stiffness, it does not necessarily have enough capacity for the stress limit. Therefore, we solve another optimization problem considering strain energy and stress constraint. The effectiveness of the proposed approach is confirmed through numerical examples, and the characteristics of the optimal shapes are discussed.

Keywords: shape optimization, Bézier curve, nonlinear programming, ruled surface.

1. Introduction

Advancement of computer technologies as well as the developments of structural materials and construction methods enabled us to design so called *free-form shell* [1–3], which has complex shape and topology that cannot be categorized to traditional shapes. Design problem of free-form shells can be naturally formulated as an optimization problem considering mechanical performances. However, to design a practically acceptable shape, non-structural performances such as cost of construction should be taken into account. Though developable surface is known as the surface which have high constructability, it cannnot represent complex shape [4].

A surface that can be swept out by moving a line in space is called *ruled surface*. Compared with developable surface, ruled surface has high degree of shape representation. Ruled surface also has high constructability for continuous shell structures because of the simplicity of mold preparation. Since members along generating lines are constructed as long straight beams, latticed shells consisting of ruled surface should also have high constructability.

Shape optimization of free-form RC shells using ruled surface is considered in the previous study [5]. In this study, a shape optimization approach is presented for free-form latticed shells using ruled surface. Boundary shape is defined using two Bézier curves, and the points with the same parameter value are connected by a line to model a ruled surface. The locations of control points of the Bézier curves are considered as design variables of the optimization problem. First, the strain energy is used to represent the mechanical performance. By minimizing strain energy under vertical loads, vertical displacement can be drastically reduced, but horizontal stiffness is not always improved. Therefore, not only vertical load but also horizontal load are considered. Additionally, since the strain energy minimized shell does not necessarily have enough capacity for the stress limit, the optimization method considering the stress constraints are applied to the strain energy minimized shell.

2. Shape representation of ruled surface

Ruled surface is defined as [6]

$$\boldsymbol{S}(u,v) = \boldsymbol{f}(u) + v\boldsymbol{g}(u) \tag{1}$$

where $\boldsymbol{f}(u)$ is the directing curve, $\boldsymbol{g}(u)$ is the direction vector of the generating line, respectively, defined with the parameter u $(0 \leq u \leq 1)$, and v $(0 \leq v \leq 1)$ is the parameter along the line. From Eq. (1), we have

$$\boldsymbol{S}(u,v) = (1-v)\boldsymbol{f}(u) + v\boldsymbol{h}(u) \tag{2}$$

where

$$\boldsymbol{g}(u) = \boldsymbol{f}(u) - \boldsymbol{h}(u) \tag{3}$$

is a curve that has the same parameter u as the basis curve; i.e., the line connection the points on $\boldsymbol{f}(u)$ and $\boldsymbol{h}(u)$ with the same parameter value turns out to be the line in the direction of $\boldsymbol{g}(u)$.

In this study, the curves $\boldsymbol{f}(u)$ and $\boldsymbol{h}(u)$ are defined using Bézier curves, and the surface is modeled by the set of lines in the direction of $\boldsymbol{g}(u)$. The kth order Bézier curve $\boldsymbol{P}_k(u)$ is defined as

$$\boldsymbol{P}_k(u) = \sum_{i=0}^{k} \boldsymbol{q}_i B_{k,i}(u) \tag{4a}$$

$$\boldsymbol{q}_i = \begin{pmatrix} q_{x,i} & q_{y,i} & q_{z,i} \end{pmatrix}^\top \tag{4b}$$

where, $\boldsymbol{q}_i$ is the coordinate vector of the ith control point, and $B_{k,i}(u)$ is the Bernstein basis function defined as

$$B_{k,i}(u) = \frac{k!}{i!(k-i)!} u^i (1-u)^{k-i} \quad (0 \leq u \leq 1 \quad i = 0, \cdots, k) \tag{5}$$

The orders of Bézier curves $\boldsymbol{f}(u)$ and $\boldsymbol{h}(u)$ are denoted by I and J, respectively (note that I and J are not necessarily the same). The control points for $\boldsymbol{f}(u)$ and $\boldsymbol{h}(u)$ are given as $\boldsymbol{q}_1, \cdots, \boldsymbol{q}_I$ and $\boldsymbol{q}_{I+1} \cdots, \boldsymbol{q}_{I+J}$, respectively. Then the ruled surface $\boldsymbol{S}(u,v)$ in Eq. (2) is defined using the Bézier curves as [7]

$$\boldsymbol{S}(u,v) = (1-v)\sum_{i=0}^{I} \boldsymbol{q}_i B_{I,i}(u) + v\sum_{i=0}^{J} \boldsymbol{q}_{I+i+1} B_{J,i}(u) \quad (0 \leq u, v \leq 1) \tag{6}$$

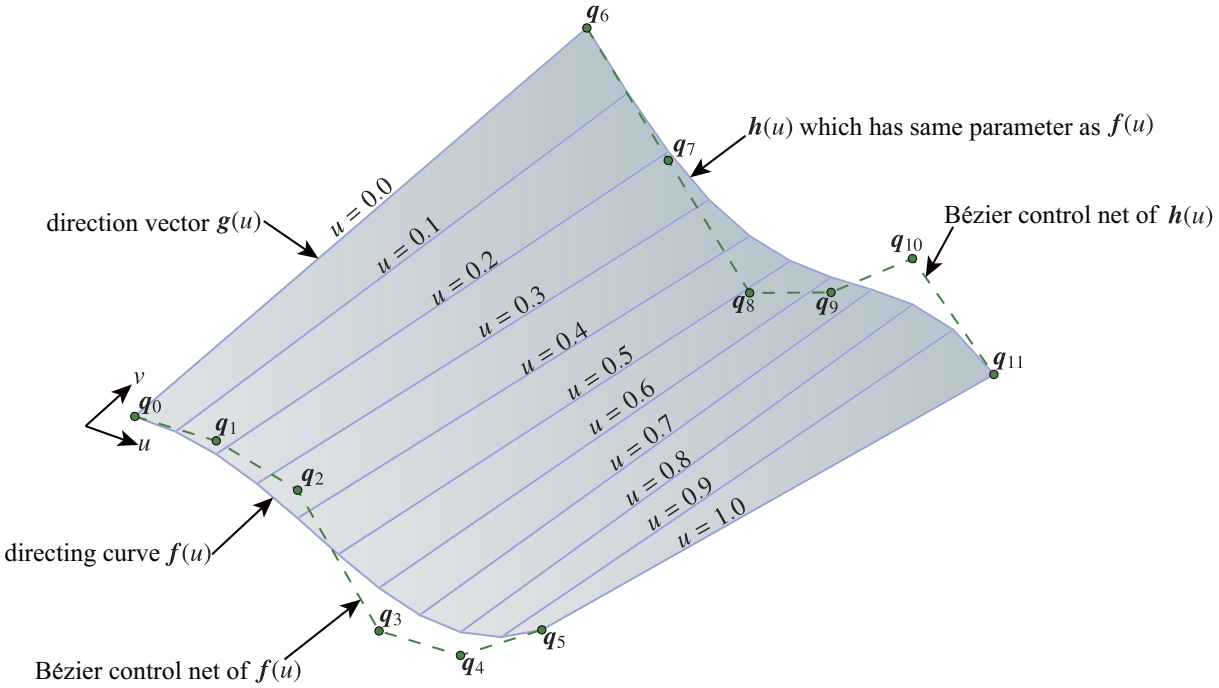

Figure 1 : Illustration of ruled surface using Bézier curves.

This way, a ruled surface is generated by assigning the coordinates of control points of the two curves on the boundary. For example, the ruled surface using Bézier curves with $I = J = 5$ is shown in Fig. 1. In order to evaluate the static responses of the latticed shells using beam elements, we divide the surface of (6) into $I' \times J'$ grid with uniformly spaced parameters u and v, respectively, and the vector $\boldsymbol{r}_x$ of the x-coordinates of the nodes is defined as

$$\boldsymbol{r}_x = \begin{pmatrix} x_{0,0} & \cdots & x_{0,I'} & \cdots & x_{I',0} & \cdots & x_{I',J'} \end{pmatrix}^\top \tag{7}$$

$\boldsymbol{r}_y$ and $\boldsymbol{r}_z$ are defined similarly. The coordinate vector of a node on the ruled surface can be written as

$$\boldsymbol{S}_{I,J}(u_k, v_l) = (1 - v_l) \sum_{i=0}^{I} \boldsymbol{q}_i B_{I,i}(u_k) + v_l \sum_{i=0}^{J} \boldsymbol{q}_{I+i+1} B_{J,i}(u_k) \quad \begin{matrix} (0 \le u_k, v_l \le 1) \\ (k = 0, \cdots, I') \\ (l = 0, \cdots, J') \end{matrix} \tag{8}$$

3. Optimization problem

The latticed shell is discretized into 3-D beam elements. Let N denote the number of degrees of freedom. The nodal displacement vector against specified static nodal load vector $\boldsymbol{P} \in \mathbb{R}^N$ is denoted by $\boldsymbol{d} \in \mathbb{R}^N$. The stiffness matrix is defined as $\boldsymbol{K} \in \mathbb{R}^{N \times N}$. We consider two types of optimization problem. The first problem is the strain energy minimization under volume constraint, and second problem is the volume minimization under stress constraint. The library pyOpt [8] is used for optimization.

3. 1. Optimization considering stiffness

Let $\boldsymbol{x}$ denote the vector of design variables consisting of coordinates of control points. To increase stiffness, the optimization problem is defined as follows:

$$\text{minimize} \quad f_1(\boldsymbol{x}) = \frac{1}{2} \boldsymbol{d}^\top \boldsymbol{K} \boldsymbol{d} \tag{9a}$$

$$\text{subject to} \quad g_1(\boldsymbol{x}) = V - \bar{V} \le 0 \tag{9b}$$

$$g_2(\boldsymbol{x}) = \bar{A} - A \le 0 \tag{9c}$$

This is the total strain energy minimization problem under the upper-bound constraint on the total material volume V (9b), and the lower-bound constraint on the horizontal projected area A (9c), where $\bar{V}$ is the upper limit of V, $\bar{A}$ is the lower limit of A.

3. 2. Optimization considering member stress

Let $\boldsymbol{a}$ denote the vector of design variables consisting of parameters of cross-sectional shape. Optimal shape of problem (9) should have high stiffness, but the local stress may not be reduced. Therefore, we solve the additional optimization problem, which minimizes the total material volume under stiffness and stress constraint as follows:

$$\text{minimize} \quad f_2(\boldsymbol{a}) = V \tag{10a}$$

$$\text{subject to} \quad f_1(\boldsymbol{a}) \le \bar{f}_1 \tag{10b}$$

$$g_3(\boldsymbol{a}) = F_{ij} - 0.90 \le 0 \quad \begin{matrix} (i = 1, \cdots, m) \\ (j = 1, 2) \end{matrix} \tag{10c}$$

where Eq. (10b) is the upper-bound constraint on the strain energy and $\bar{f}_1$ is upper limit of f_1. F_{i1} and F_{i2} are the allowable stress ratios at two ends of ith beam, which is defined by Japanese design code as

follows (note that this equation is for use in steel pipe) [9]:

$$F_{ij} = \begin{cases} \dfrac{\sigma_{c,ij}}{f_{c,ij}} + \dfrac{\sigma_{b,ij}}{f_{b,ij}} & \cdots \text{if} \quad N_{ij} > 0 \\ \dfrac{\sigma_{t,ij}}{f_{t,ij}} + \dfrac{\sigma_{b,ij}}{f_{b,ij}} & \cdots \text{if} \quad N_{ij} \leq 0 \end{cases} \quad \begin{matrix} (i = 1, \cdots, m) \\ (j = 1, 2) \end{matrix} \tag{11a}$$

$$\sigma_{c,ij}, \sigma_{t,ij} = \frac{|N_{ij}|}{A_{ij}}, \quad \sigma_{b,ij} = \frac{\sqrt{M_{z,ij}^2 + M_{y,ij}^2}}{Z_i} \tag{11b}$$

$$f_t = f_b = F/1.5, \quad f_c = \begin{cases} \dfrac{1 - 0.4(\lambda/\Lambda)^2}{\nu} & \cdots \text{if } \lambda \leq \Lambda \\ \dfrac{0.277F}{(\lambda/\Lambda)^2} & \cdots \text{if } \lambda > \Lambda \end{cases} \tag{11c}$$

$$\Lambda = \sqrt{\frac{\pi^2 E}{0.6F}}, \quad \nu = \frac{3}{2} + \frac{2}{3}(\lambda/\Lambda)^2 \tag{11d}$$

where m is the number of members, A_i and Z_i are the cross-sectional area and the section modulus of ith member, N_{ij}, $M_{z,ij}$ and $M_{y,ij}$ are the axial force and the bending moments with respect to y- and z-axes at jth end of member i, respectively. f_c, f_t, f_b are the allowable compressive/tensile/bending stress, λ, Λ, E, F are the slenderness ratio of the compression member, critical slenderness ratio, Young's modulus, design strength of steel, respectively. In the case of short-term loading, the allowable compressive/tensile/bending stress are multiplied by 1.5, respectively. To avoid a low safety design, F_{ij} is constrained to 0.9 or less.

4. Design load

As a permanent load, 290N/m^2 surface load is considered as the roof cladding in addition to their self-weight. Let n denote the number of nodes, and the vertical components of the equivalent nodal force of the permanent load are denoted as $w_i (i = 1, \cdots, n)$. As a seismic load, concentrated loads of $0.3w_i$ are applied to each node in the X and Y directions. Each load is indicated by L, X, and Y. For example, in the case of the permanent load, strain energy is denoted as $f_1^{(L)}$.

5. Latticed shell model consisting of ruled surface

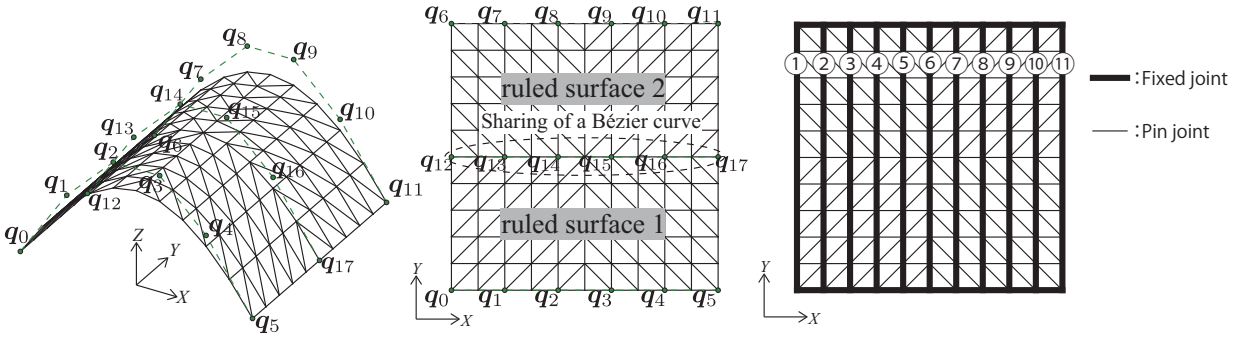

(a) Isometric (b) Plan (c) Joint condition

Figure 2 : Latticed shell model

In general, a surface consisting of a single ruled surface can express only a few kinds of shapes. But a piecewise ruled surface can represent various shapes as compared with a single ruled surface. In this paper, the analytical model of the latticed shell which consists of two connected ruled surfaces as shown Fig.2 is considered for the initial shape of the optimization problems. Two ruled surfaces which are defined by the Eq.(6) have two respective Bézier curves and one jointly Bézier curve. Each Bézier curve has 6 control points (18 points in total). The x, y, and z coordinate vectors of the control points are defined as $\boldsymbol{q}_x$, $\boldsymbol{q}_y$, $\boldsymbol{q}_z$, respectively.

Table 1 : Elastic analysis result of initial model

Load case	A [m^2]	f_1 [kNm]	V [kN]	$d_x^{\max}$ [mm]	$d_y^{\max}$ [mm]	$d_z^{\max}$ [mm]	$N_c^{\max}$ [kN]	$N_t^{\max}$ [kN]	$M^{\max}$ [kNm]	$Q^{\max}$ [kNm]	Load case	$F_{ij}^{\max}$
L	2500	192.8	16.70	1574	10.76	1187	1225	583.7	347.8	39.74	L	5.01
X		547.3		2247	4.799	1840	515.4	515.4	740.4	90.39	$L \pm X$	8.47
Y		1.964		49.35	13.84	49.98	131.2	131.2	38.71	8.422	$L \pm Y$	3.43

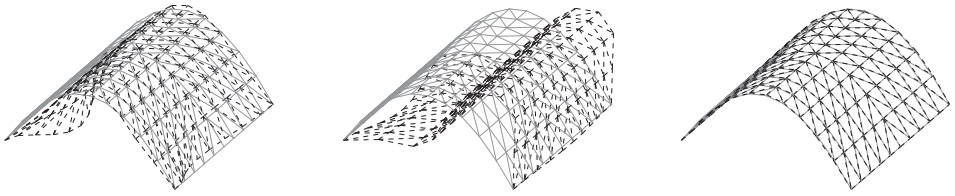

(a) load case L (b) load case X (c) load case Y

Figure 3 : Displacement distribution of initial model

The parameter values for the nodes of each ruled surface are uniformly spaced as $u_i = 0.0, 0.1, \cdots, 1.0$ and $v_i = 0.0, 0.1, \cdots, 1.0$. The span is 50m in both of x- and y-directions and the height is 20m, respectively. The material of members is steel with Young's modulus 210 GPa, Poisson's ratio 0.3, and design strength 235N/mm^2, respectively. Displacement is fixed at the four corners. The values of n, N, and m are 121, 702, and 320, respectively. All members have the same cross-sectional shape, which is the steel pipe with outside diameter 267.4mm and thickness 9.0mm.

For the constructability, it is desirable that the members in the v-direction consist of a long straight beam. In order to reduce the welding on site, the two ends of the members in u-direction except those along the outer circumference are connected using pin joints as shown in Fig.2(c).

The results of elastic analysis for load cases L, X, and Y are listed in Table 1, where $d_x^{\max}$, $d_y^{\max}$, $d_z^{\max}$ $N_t^{\max}$, $N_c^{\max}$, $Q^{\max}$, $M^{\max}$, and $F_{ij}^{\max}$ are the maximum values of global x- y- z-directional nodal displacement, tensile axial force, compressive axial force, shear force, bending moment, and allowable stress ratio in each load case, respectively. Note that $Q^{\max}$ and $M^{\max}$ are calculated as $Q^{\max} = \sqrt{(Q^{\max})_y^2 + (Q_z^{\max})^2}$ and $M^{\max} = \sqrt{(M^{\max})_y^2 + (M_z^{\max})^2}$, where $Q_y^{\max}$, $Q_z^{\max}$, $M_y^{\max}$, and $M_z^{\max}$ are the maximum values of global y- z-directional shear force and bending moment around the local y- and z- axis, respectively. The stress values of load cases $L+X$, $L-X$, $L+Y$, and $L-Y$ are calcuated by using the elastic analysis results of L, X, and Y. Note that the values of $L \pm X(Y)$ in Table 1 represent the larger values of the cases $L+X(Y)$ and $L-X(Y)$. In the calculation of allowable stress ratio, all load cases except for L are defined as short-term loading. The dashed lines and gray solid lines in Fig. 3 are undeformed and deformed shapes of the initial model, respectively, where the displacements are magnified by the factor 5.

It can be confirmed from these results that the initial shape has small stiffness in vertical and x directions and the maximum allowable stress ratio is far larger than the upper bound 0.9.

6. Optimization for stiffness

First, we consider the optimization problem (9), where constraint (9c) is not required because A is constant. The values of initial model are assigned for $\bar{V}$ and $\bar{A}$ as $\bar{V}$=16.70m^3 and $\bar{A}$=2500m^2.

6. 1. Optimization under vertical load

Optimization problem for long-term load is formulated as follows:

$$\begin{aligned} &\text{minimize} && f_1^{(L)}(\boldsymbol{q}_z^*) && \text{(12a)} \\ &\text{subject to} && g_1(\boldsymbol{q}_z^*) \leq 0 && \text{(12b)} \end{aligned}$$

where $\boldsymbol{q}_z^*$ is the design variable vector that is defined by removing the fixed values $q_{z,0}$, $q_{z,5}$, $q_{z,6}$, and $q_{z,11}$ from $\boldsymbol{q}_z$ as

Table 2 : Elastic analysis result of optimal shape of problem (12)

Load case	A [m^2]	f_1 [kNm]	V [kN]	$d_x^{\max}$ [mm]	$d_y^{\max}$ [mm]	$d_z^{\max}$ [mm]	$N_c^{\max}$ [kN]	$N_t^{\max}$ [kN]	$M^{\max}$ [kNm]	$Q^{\max}$ [kNm]	Load case	$F_{ij}^{\max}$
L	2500	6.871	16.70	18.95	22.53	29.68	282.7	89.72	29.69	11.12	L	0.60
X		535.9		2251	123.5	1674	855.4	855.3	485.1	94.09	$L \pm X$	4.38
Y		35.16		117.7	138.8	158.9	503.8	503.8	113.0	24.54	$L \pm Y$	1.18

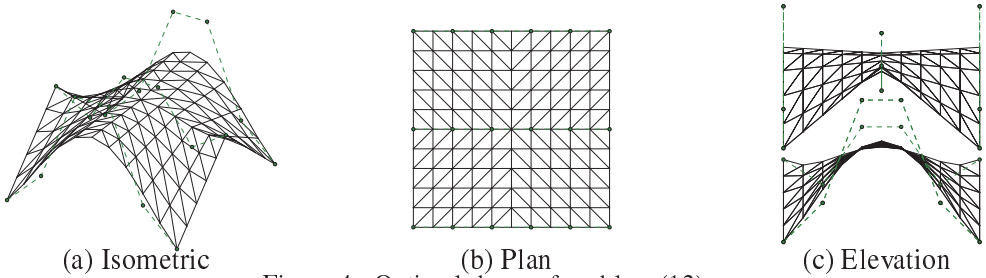

(a) Isometric (b) Plan (c) Elevation

Figure 4 : Optimal shape of problem (12)

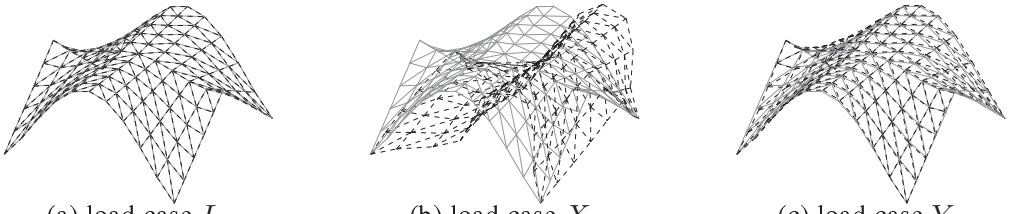

(a) load case L (b) load case X (c) load case Y

Figure 5 : Displacement distribution of optimal shape of problem (12)

$$\boldsymbol{q}_z^* = \begin{pmatrix} q_{z,1} & \cdots & q_{z,4} & q_{z,7} & \cdots & q_{z,10} & q_{z,13} & \cdots & q_{z,16} \end{pmatrix} \tag{13}$$

The result of elastic analysis for optimal shape to each load case of L, X, and Y is listed in Table 2. The optimal shape is shown in Fig. 4. The dashed lines and gray solid lines in Fig. 5 are undeformed and deformed shapes, where the displacements are magnified by the factor 5.

It can be confirmed from the optimization result that the bending moments in the load case L are drastically reduced and the vertical stiffness is drastically increased. However, in other load cases, the optimal shape has unacceptably large stresses in members and has small x-directional stiffness.

6. 2. Optimization under vertical and horizontal loads

In order to improve x-directional stiffness, we next consider the following optimization problem:

$$\begin{aligned} \text{minimize} \quad & f_1^{(L)}(\boldsymbol{q}_y^*, \boldsymbol{q}_z^*) + f_1^{(X)}(\boldsymbol{q}_y^*, \boldsymbol{q}_z^*) + f_1^{(Y)}(\boldsymbol{q}_y^*, \boldsymbol{q}_z^*) && \text{(14a)} \\ \text{subject to} \quad & g_1(\boldsymbol{q}_y^*, \boldsymbol{q}_z^*) \leq 0 && \text{(14b)} \\ & g_2(\boldsymbol{q}_y^*, \boldsymbol{q}_z^*) \leq 0 && \text{(14c)} \end{aligned}$$

In this case, the values of strain energy for load cases X and Y are added to the objective function of problem (12). To expand feasible region, $\boldsymbol{q}_y^*$, which is defined similarly to $\boldsymbol{q}_z^*$, is also included in design variable.

The results of elastic analysis for optimal shape to each load case of L, X, and Y is listed in Table 3. The optimal shape is shown in Fig.6. The dashed lines and gray solid lines in Fig. 7 are undeformed and deformed shapes, where the displacements are magnified by the factor 5.

It can be confirmed from the optimization results that the bending moments not only in the load case L but also in the load cases X and Y are drastically reduced and the vertical and horizontal stiffnesses are simultaneously increased. The shape is changed in both vertical and horizontal directions while A is constrained to $\bar{A}$. To reduce the overturning moment, the rise of optimal shape is not very large and the volume constraint is inactive. The member stresses in all cases are drastically reduced; however, the allowable stress ratios in the load case $L + X$ are still unacceptable ($F_{ij}^{\max^{(L+X)}} \geq 1$) and the optimal shape has low safety factor for load case L ($F_{ij}^{\max^{(L)}} \geq 0.9$).

Table 3 : Elastic analysis result of optimal shape of problem (14)

Load case	A [m^2]	f_1 [kNm]	V [kN]	$d_x^{\max}$ [mm]	$d_y^{\max}$ [mm]	$d_z^{\max}$ [mm]	$N_c^{\max}$ [kN]	$N_t^{\max}$ [kN]	$M^{\max}$ [kNm]	$Q^{\max}$ [kNm]	Load case	$F_{ij}^{\max}$
L	2500	15.76	15.72	26.92	13.33	52.05	525.9	252.4	56.08	18.92	L	0.96
X		4.010		37.78	14.35	38.47	389.8	390.0	44.22	13.30	$L \pm X$	1.06
Y		3.665		46.26	49.36	76.32	146.0	142.2	41.79	11.13	$L \pm Y$	0.76

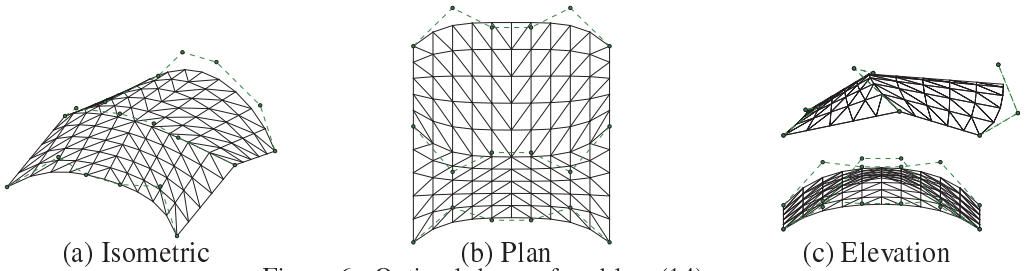

(a) Isometric (b) Plan (c) Elevation

Figure 6 : Optimal shape of problem (14)

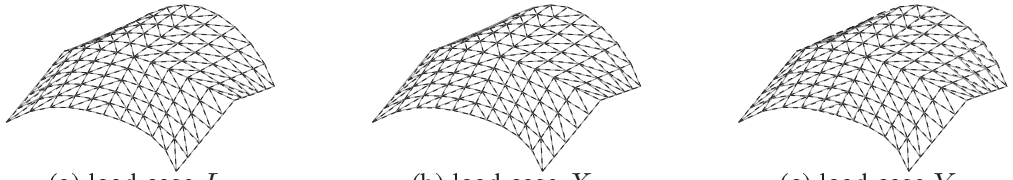

(a) load case L (b) load case X (c) load case Y

Figure 7 : Displacement distribution of optimal shape of problem (14)

7. Optimization for stress

Next, we consider the optimization problem (10). To reduce the member stresses while maintaining high stiffness, the optimal shape of problem(14) is selected as the initial model of the optimization problem (10). The values of initial model are assigned for $\bar{A}$ and $\bar{f}_1$ as $\bar{A}$ =2500m^2 and $\bar{f}_1$ =20kNm. About the cross-sectional shape, outside diameter values of each member are defined as $\boldsymbol{R} = \begin{pmatrix} R_1 & \cdots & R_m \end{pmatrix}$.

In this paper, cross-sectional shape of all members is a circular steel tube. In order to express cross-sectional properties as a outside diameter only, R/t is fixed to 27.5 (the average ratio of the circulation steel pipe). To avoid a member vanishment or appearing over-sized members, the range of R_i is specified as 100mm $\leq R_i \leq$ 1000mm $(i = 1, \cdots, m)$. For the constructability, it is desirable that the members of the v direction have same cross-sectional shape, so we sort the members of the v direction into 11 groups as shown in Fig.2(c) and outside diameter values are made equal each other in the groups.

Based on the above, the following optimization problem is considered:

$$\text{minimize} \quad f_2(\boldsymbol{R}^*) \tag{15a}$$

$$\text{subject to} \quad f_1^{(L)}(\boldsymbol{R}^*) + f_1^{(X)}(\boldsymbol{R}^*) + f_1^{(Y)}(\boldsymbol{R}^*) \leq \bar{f}_1 \tag{15b}$$

$$g_3(\boldsymbol{R}^*)^{(L)} \leq 0 \tag{15c}$$

$$g_3(\boldsymbol{R}^*)^{(L+X)} \leq 0 \tag{15d}$$

$$g_3(\boldsymbol{R}^*)^{(L-X)} \leq 0 \tag{15e}$$

$$g_3(\boldsymbol{R}^*)^{(L+Y)} \leq 0 \tag{15f}$$

$$g_3(\boldsymbol{R}^*)^{(L-Y)} \leq 0 \tag{15g}$$

where $\boldsymbol{R}^*$ is the vector which reduced the number of the design variable from $\boldsymbol{R}$ by using member grouping. Note that the elastic analysis is done in the case of L, X, and Y only and the mechanical values of other combination load cases are calculated by using the analysis result in the case of L, X, and Y.

Table 4 : Elastic analysis result of optimal shape of problem (15)

Load case	A [m^2]	f_1 [kNm]	V [kN]	$d_x^{\max}$ [mm]	$d_y^{\max}$ [mm]	$d_z^{\max}$ [mm]	$N_c^{\max}$ [kN]	$N_t^{\max}$ [kN]	$M^{\max}$ [kNm]	$Q^{\max}$ [kNm]	Load case	$F_{ij}^{\max}$
L	2500	13.35	5.229	43.00	24.83	84.99	312.1	169.1	46.63	13.39	L	0.90
X		3.779		57.40	26.08	72.78	212.2	212.4	51.26	11.76	$L \pm X$	0.90
Y		2.869		65.25	60.84	90.44	92.43	88.30	49.14	10.57	$L \pm Y$	0.90

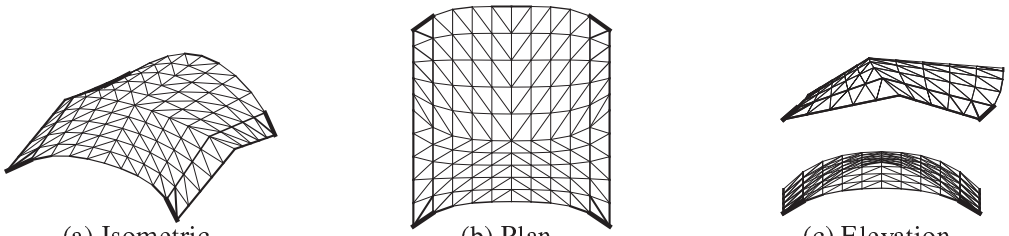

(a) Isometric (b) Plan (c) Elevation

	①	②	③	④	⑤	⑥	⑦	⑧	⑨	⑩	⑪	other members
R[mm]	309.4	272.8	189.6	175.7	141.6	112.8	112.8	171.6	197.6	277.1	298.8	100.0～507.5

Figure 8 : Optimal shape and area destribution of problem (15)

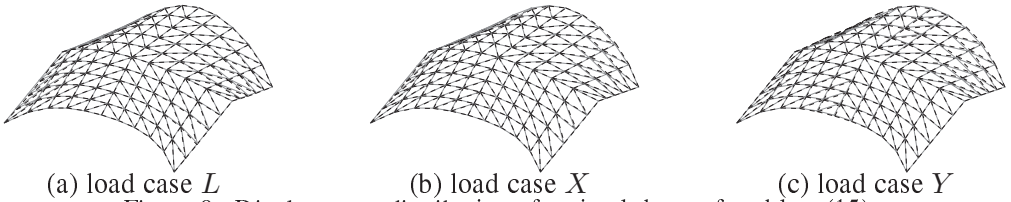

(a) load case L (b) load case X (c) load case Y

Figure 9 : Displacement distribution of optimal shape of problem (15)

The results of elastic analysis for optimal shape to each load case of L, X, and Y is listed in Table 4. The line width in Fig.8 represents the magnitude of the cross-sectional area. The dashed lines and gray solid lines in Fig.9 are undeformed and deformed shapes, where the displacements are magnified by the factor 5.

It can be confirmed from the optimization results that all the load cases of the allowable stress ratios are reduced to 0.90 or less while reducing the total material volume and maintaining the high stiffness.

8. Conclution

The main conclusions are given below.

1. Various shapes can be easily defined by small number of parameters by using a pair of Beźier curves for boundary shape of ruled surface.

2. the variety of shape can be enhanced by connecting several ruled surfaces.

3. Optimization for minimum strain energy dors not always reduce member stresses, which can be reduced by optimization considering cross-sectional shapes as the design variables.

4. Since all of the optimal solutions obtained in this paper are ruled surfaces, these latticed shells have high constructability compared to general latticed shells with free-form surface.

Acknowledgment

This work is partially supported by JSPS KAKENHI Grant No. 16K14338.

References

[1] E. Ramm, K.-U. Bletzinger and R. Reitinger, Shape optimization of shell structures, *Bulletin of Int. Assoc. for Shell and Spatial Struct.*, 1993, Vol. 34(2), pp. 103–121

[2] S. Guillet, F. Noël, and J. C. Léon, Structural shape optimization of parts bounded by free-form surfaces, *StrOpt*, 1996, Vol. 11, pp. 159–169

[3] J. Wu and R. Burgueno, An integrated approach to shape and laminate stacking sequence optimization of free-form FRP shells, *Computer Methods in Applied Mechanics and Eng.*, 2006, Vol. 195, pp. 4106–4123

[4] S. Fujita and M. Ohsaki, Shape Optimization of Free-form Shells Using Invariants of Parametric Surface, *International Journal of Space Structures*, 2010, Vol. 25, No.3, pp. 143–157

[5] K. Seki, M. Ohsaki and S. Fujita, Shape optimization of ruled surface considering static stiffness, *11th Asian Pacific Conference on Shell and Spatial Structures*, 2015, pp. 269–274

[6] G.W.M. Kallenberg, Ruled surfaces in a particular geometry, *Indagationes Mathematicae (Proceedings)*, 1960, Vol. 63, pp. 291–296

[7] H. Pottmann and J. Wallner, Computational Line Geometry, Springer, 2001.

[8] R. E. Perez, P. W. Jansen, and J. R. R. A. Martins: pyOpt, A Python-Based Object-Oriented Framework for Nonlinear Constrained Optimization, *Structures and Multidisciplinary Optimization*, 2012, Vol. 45, No.1, pp. 101–118

[9] Architectural Institute of Japan, Design Standard for Steel Structures –Based on Allowable Design Concept–, 2005.